American Journal of Applied Mathematics
2022; 10(5): 212-222
http://www.sciencepublishinggroup.com/j/ajam
doi: 10.11648/j.ajam.20221005.13
ISSN: 2330-0043 (Print); ISSN: 2330-006X (Online)

Heat and Mass Transfer Effects on Unsteady Magnetohydrodynamics Stokes Free-Convective Flow Past an Infinite Vertical Porous Plate in a Rotating System

Mayaka Augustine Ayanga*, Mathew Ngugi Kinyanjui, Jeconia Okelo Abonyo, Johana Kibet Sigey

Department of Pure and Applied Mathematics, Jomo Kenyatta University of Agriculture and Technology, Nairobi, Kenya

Email address:

ayangaaugustine@gmail.com (Mayaka Augustine Ayanga), mathewkiny@jkuat.ac.ke (Mathew Ngugi Kinyanjui), masenooj@gmail.com (Jeconia Okelo Abonyo)

*Corresponding author

To cite this article:

Mayaka Augustine Ayanga, Mathew Ngugi Kinyanjui, Jeconia Okelo Abonyo, Johana Kibet Sigey. Heat and Mass Transfer Effects on Unsteady Magnetohydrodynamics Stokes Free-Convective Flow Past an Infinite Vertical Porous Plate in a Rotating System. *American Journal of Applied Mathematics*. Vol. 10, No. 5, 2022, pp. 212-222. doi: 10.11648/j.ajam.20221005.13

Received: August 30, 2022; **Accepted**: October 12, 2022; **Published**: October 24, 2022

Abstract: In this paper, Stokes first problem for an unsteady MHD free convective flow of a viscous incompressible fluid past an infinite vertical porous plate in the presence of a transverse variable magnetic field in a rotating system has been studied. The dimensionless governing partial differential equations are solved numerically by the finite difference method based on the forward-time central-space scheme. The resulting difference equations are simulated in MATLAB software to obtain the profiles of the flow variables. The skin-friction coefficient and the rates of heat and mass transfer are also computed. The simulation results are presented graphically and in tabular forms, and also discussed. The main findings are that an increase in the joule heating parameter results in a uniform increase in the velocity and temperature profiles near the plate but remain constantly distributed away from the plate. This observation implies that the flow is influenced substantially by the strength of joule heating near the plate and in the bulk of the fluid. The results obtained in this study regarding thermal and mass diffusion effects can be applied in the industry, for instance, in the separation of isotopes contained in a mixture of very light molecular-weight gases (for instance, hydrogen and helium) and medium molecular-weight gases (for instance, nitrogen and air).

Keywords: MHD-Flow, Rotating-System, Stokes-Problem, Vertical-Porous-Plate, Variable-Magnetic-Field, Skin-Friction, Heat-Transfer, Mass-Transfer

1. Introduction

The theory of rotating fluids is important because of its occurrence in various natural phenomena and technological situations, which are directly governed by the action of Coriolis force on the flow. There has been considerable interest in the study of MHD flows in rotating systems due to their applications in geophysics, astrophysics and in turbo machines. This study is on investigating the Stokes first problem for the unsteady hydromagnetic free convective flow of a viscous incompressible fluid past an infinite vertical porous plate subjected to suction in the presence of a transverse variable magnetic field.

The MHD flow of fluids through porous materials is of interest, for instance, to the hydrologist, who is concerned with the study of underground water seepage; and to the petroleum engineer, who is interested in the flow of oil and gas through the reservoir. Research on fluid flows through porous materials in the presence of magnetic field has been applied extensively in the manufacturing of computer disk drives and various machines used in the industry. In water storage and treatment systems, saturated porous materials are widely used to insulate the storage tanks so as to control the rates of heat and mass transfer. The underground water pipes are also insulated to prevent the water in the pipes from freezing during winter.

There are various theoretical studies in modeling the fluid flow past an infinite vertical porous plate. For example, O. D. Makinde and A. Ogulu [1] studied the effect of temperature-dependent viscosity on steady free convective

flow past an infinite vertical porous plate in the presence of a transverse magnetic field, thermal radiation, and a first-order homogeneous chemical reaction. The model equations were solved numerically by the shooting method. The results obtained from the study revealed that when the viscosity of an electrically conducting fluid is sensitive to the difference in temperature between the plate and the ambient fluid in the presence of a magnetic field, thermal radiation, and chemical reaction, then the variable viscosity effect must be considered. Also, for cooling of the plate by free convection currents, the rate of mass transfer increases with increasing values of the reaction parameter and the Schmidt number. The skin-friction coefficient increases with increasing values of the viscosity variation parameter but decreases with increasing values of the magnetic Hartmann number.

Prakash *et al.* [2] studied Dufour and radiation effects on Stokes first problem for the unsteady two-dimensional MHD free convection flow past an infinite vertical porous plate with variable temperature and uniform mass diffusion in the presence of a uniform transverse magnetic field. The model equations were solved analytically by the method of Laplace transform. The results revealed that an increase in Hartmann number impedes the velocity of the fluid when the plate is cooling and a reverse effect was observed for a heated plate. Also, an increase in the radiation parameter, Dufour number, and Grashof number accelerate the flow when the plate is cooling. Moreover, radiation parameter and Prandtl number lower the temperature but enhance the rate of heat transfer. Schmidt number decreases the concentration of the species.

Narahari *et al.* [3] studied unsteady two-dimensional MHD free convection flow of a radiative fluid past an infinite vertical plate with constant heat and mass flux in the presence of thermal radiation and uniform magnetic field. The model equations were solved analytically by the method of Laplace transform. The results obtained from the study revealed that the fluid velocity increases with an increase in the radiation parameter and decreases with an increase in the Hartmann number. This study neglected the effects of inertia on the boundary layer flow.

Murthy *et al.* [4] studied Stokes first problem for the unsteady MHD natural convective flow past an infinite vertical porous plate with thermal radiation, Hall current, heat and mass transfer in presence of transverse magnetic field of uniform strength. The model equations were solved both numerically by the finite element method and analytically by the perturbation technique. The results revealed that Hall current accelerates flow in the boundary layer region but decelerates the primary fluid velocity in the free-stream region. Further, thermal radiation accelerates both the primary and secondary velocities. Hall current and thermal radiation reduce the primary skin-friction but increase the secondary skin-friction. Moreover, the rate of heat transfer decreases with an increase in thermal radiation parameter.

Raju [5] investigated the Soret and Dufour effects on Stokes first problem for the unsteady two-dimensional MHD free convective flow of a chemically reacting fluid past an infinite vertical porous plate with heat and mass transfer in the presence of a uniform transverse magnetic field. The plate was subjected to a time-dependent suction velocity. The resulting model equations were solved numerically by the finite element method (FEM). The results revealed that the temperature of the fluid decreases with increasing radiation. The velocity was found to decrease with an increase in Hartmann number, which was attributed to the magnetic pull of the Lorentz force acting on the flow field. Moreover, the species concentration decreases with an increase in the values of Schmidt number while Soret number enhances species diffusion. The velocity and concentration profiles decrease with an increase in the chemical reaction parameter. The chemical reaction parameter and Schmidt number enhance the rate of mass transfer.

Pattnaik *et al.* [6] investigated the Dufour effect with Hall current on unsteady hydromagnetic free convection flow past an infinite vertical porous plate in the presence of a uniform transverse magnetic field subjected to a time-dependent suction or blowing velocity. The model equations were solved analytically by applying a special function. The results revealed that suction velocity induces back-flow in conjunction with opposing buoyancy forces. Also, the Hall current contributes to greater skin friction at the plate. Injection accelerates the flow and a specific layer of fluid becomes independent of Dufour effect in the presence of injection. Further, the Hall current slightly increases the velocity in the case of a steady temperature and concentration but decreases for unsteady temperature and concentration. The thermal boundary layer is thinner under the influence of suction but thicker for injection. The application of magnetic field reduces the shear stress at the plate in the case of uniformly time varying plate temperature.

Krishna *et al.* [7] investigated the effects of Hall current on Stokes first problem for the unsteady MHD natural convective flow of second grade fluid past an infinite vertical porous plate with heat and mass transfer in a rotating frame of reference. The study considered a uniform transverse magnetic field. The resulting system of linear partial differential equations were solved analytically by the method of Laplace transform. The results obtained from the study revealed that Hall current and rotation accelerate the secondary velocity and decelerate the primary velocity. Also, the flow accelerates with time. Further, thermal radiation and thermal diffusion enhance the temperature of the fluid while mass diffusion enhances the species concentration. Rotation parameter and second-grade fluid parameter enhance the shear stress at the plate. Also, thermal radiation parameter reduces the rate of heat transfer.

Finally, theoretical studies in modeling the MHD fluid flow in different flow configurations have also drawn the attention of many authors [3, 8-16].

From the above previous modeling studies on fluid flow past an infinite vertical porous plate, it is noted that variable magnetic field, magnetic induction, joule heating, viscous dissipation, and rotating system have received little attention. The identified research gaps prevent the direct application of existing models to the sheeting industry. Therefore, the present study seeks to generalize the results of Krishna *et al.*

[7] to include the effects of variable magnetic field, magnetic induction, joule heating, viscous dissipation, chemical reaction, heat source, Soret and Dufour effects for the case of a nonelastic fluid. The study results are essential in the sheeting industry and in the design of engineering devices which operate on the principles of MHD flow.

2. Mathematical Modeling

In this study, the unsteady MHD Stokes free convection flow of a viscous incompressible fluid past an infinite vertical porous plate subjected to variable suction is considered, as shown in Figure 1. A Cartesian coordinate system (x, y, z) *is chosen such that x-axis is along the plate in the vertically upward direction, y-axis is normal to the plate and $z-$axis is along the width of the plate (i.e., perpendicular to the* xy*-plane). The plate is infinite in extent in both* x *and* z *directions, so the domain under consideration is* $-\infty < x < \infty$, $0 \le y < \infty$ *and* $-\infty < z < \infty$.

The plate and the fluid rotate as a rigid body with a constant angular velocity Ω *about the y-axis. A strong magnetic field* $\tilde{\mathrm{H}}$ *of variable strength* H *is applied along the y-axis. At time* $t \le 0$, *the plate and the fluid are assumed to have the same uniform temperature* T_∞ *and the strength of the imposed magnetic field is* H_0. *At time* $t > 0$, *the plate starts moving impulsively along the positive x-axis with a uniform velocity* $U_0 > 0$ *and its temperature is instantaneously lowered or raised to* T_{wall}, *which is maintained constant thereafter. The species concentration at the plate is* C_{wall} *while that at the free-stream is* C_∞.

Since the applied magnetic field is strong, the Hall current significantly affects the flow. The effect of Hall current gives rise to a force in a direction perpendicular to the xy-plane (i.e., in the z-direction), which induces a cross flow in that direction and hence the flow becomes three-dimensional. Since the plate is infinite in extent in both x and z directions and the flow is unsteady, the flow variables in this study are functions of y and t only. Since the applied magnetic field is of variable strength, its magnitude (H) is also a function of y and t.

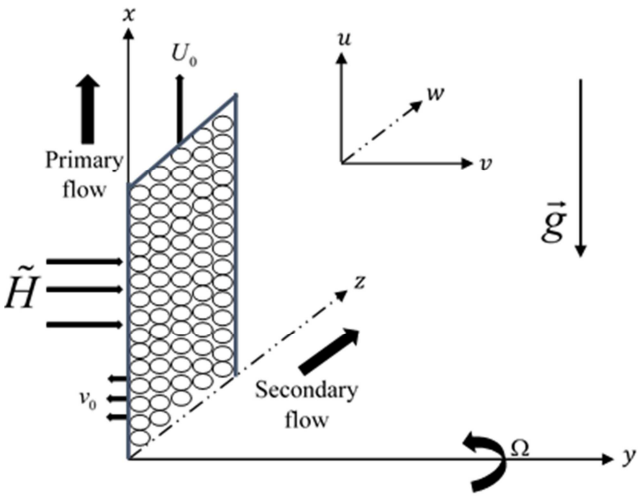

Figure 1. *Geometry of the research problem.*

2.1. Governing Equations

Under the assumption that all the fluid properties are constants, there is no-slip condition at the plate, the fluid is electrically conducting and the plate is non-conducting, the governing equations of continuity, momentum, energy, concentration, and magnetic induction are given as:

$$\frac{\partial v}{\partial y} = 0 \quad \Rightarrow \quad v = -v_0\left(1+\epsilon e^{nt}\right) \tag{1}$$

$$\rho\left[\frac{\partial u}{\partial t} + v\frac{\partial u}{\partial y} + 2\Omega w\right] = -\frac{\mu}{\kappa}u + \mu\frac{\partial^2 u}{\partial y^2} + \rho g\beta_T(T-T_\infty) + \rho g\beta_C\left(C-C_\infty\right) - \frac{\sigma\mu_e^2 H_0^2\sqrt{H_x^2+H_0^2}\left[\sqrt{H_x^2+H_0^2}u + mH_0 w\right]}{\left[H_x^2+H_0^2\left(1+m^2\right)\right]} \tag{2}$$

$$\rho\left[\frac{\partial w}{\partial t} + v\frac{\partial w}{\partial y} - 2\Omega u\right] = -\frac{\mu}{\kappa}w + \mu\frac{\partial^2 w}{\partial y^2} + \frac{\sigma\mu_e^2 H_0^2\sqrt{H_x^2+H_0^2}\left[mH_0 u - \sqrt{H_x^2+H_0^2}w\right]}{\left[H_x^2+H_0^2\left(1+m^2\right)\right]} \tag{3}$$

$$(\rho Cp)\left[\frac{\partial T}{\partial t} + v\frac{\partial T}{\partial y}\right] = k\left(1+\frac{16\sigma_0 T_\infty^3}{3k_0 k}\right)\frac{\partial^2 T}{\partial y^2} + \mu\left[\left(\frac{\partial u}{\partial y}\right)^2 + \left(\frac{\partial w}{\partial y}\right)^2\right] + Q_0\left(T-T_\infty\right) + \frac{\sigma\mu_e^2 H_0^2\left(H_x^2+H_0^2\right)}{\left[H_x^2+H_0^2\left(1+m^2\right)\right]}\left(u^2+w^2\right) + \frac{\rho D_m K_T}{C_S}\frac{\partial^2 C}{\partial y^2} \tag{4}$$

$$\frac{\partial C}{\partial t} + v\frac{\partial C}{\partial y} = D_m\frac{\partial^2 C}{\partial y^2} - K_r\left(C-C_\infty\right) + \frac{D_m K_T}{T_m}\frac{\partial^2 T}{\partial y^2} \tag{5}$$

$$\frac{\partial H_x}{\partial t} = H_0 \frac{\partial u}{\partial y} + D_{\mathrm{B}} \frac{\partial^2 H_x}{\partial y^2} \tag{6}$$

subject to the following initial and boundary conditions, for $y \geq 0$ and $t \geq 0$.

$$u = 0, w = 0, T = T_\infty, C = C_\infty, H_x = 0 \quad \text{at } t = 0 \tag{7}$$

$$u = U_0, w = 0, T = T_{\mathrm{wall}}, C = C_{\mathrm{wall}}, H_x = H_0 \text{ at } y = 0 \tag{8}$$

$$u = 0, w = 0, T = T_\infty, C = C_\infty, H_x = 0 \text{ as } y \to \infty \tag{9}$$

The dimensionless variables are introduced as follows:

$$\overline{y} = \frac{y}{\mu/(\rho U_0)}, \overline{t} = \frac{t}{\mu/(\rho U_0^2)}, \overline{n} = \frac{n}{\left(\rho U_0^2\right)/\mu} \tag{10}$$

$$\overline{u} = \frac{u}{U_0}, \overline{v} = \frac{v}{U_0}, \overline{w} = \frac{w}{U_0}, \overline{v}_0 = \frac{v_0}{U_0} \tag{11}$$

$$\theta = \frac{T - T_\infty}{T_{\mathrm{wall}} - T_\infty}, \phi = \frac{C - C_\infty}{C_{\mathrm{wall}} - C_\infty}, h = \frac{H_x}{H_0} \tag{12}$$

The chain rule of differentiation yields the dimensionless forms of the specific governing equations as:

$$\frac{\partial \overline{v}}{\partial \overline{y}} = 0 \quad \Rightarrow \quad \overline{v} = -\overline{v}_0 \left(1 + \epsilon e^{\overline{n}\overline{t}}\right) \tag{13}$$

$$\frac{\partial \overline{u}}{\partial \overline{t}} + \overline{v}\frac{\partial \overline{u}}{\partial \overline{y}} + 2\mathrm{R}_{\mathrm{o}}\overline{w} = -\frac{1}{\mathrm{K}}\overline{u} + \frac{\partial^2 \overline{u}}{\partial \overline{y}^2} + \mathrm{Gr}_{\mathrm{T}}\theta + \mathrm{Gr}_{\mathrm{C}}\phi - \mathrm{M}^2 \frac{\sqrt{h^2+1}\left[\sqrt{h^2+1}\overline{u} + m\overline{w}\right]}{\left[h^2 + \left(1+m^2\right)\right]} \tag{14}$$

$$\frac{\partial \overline{w}}{\partial \overline{t}} + \overline{v}\frac{\partial \overline{w}}{\partial \overline{y}} - 2\mathrm{R}_{\mathrm{o}}\overline{u} = -\frac{1}{\mathrm{K}}\overline{w} + \frac{\partial^2 \overline{w}}{\partial \overline{y}^2} + \mathrm{M}^2 \frac{\sqrt{h^2+1}\left[m\overline{u} - \sqrt{h^2+1}\overline{w}\right]}{\left[h^2 + \left(1+m^2\right)\right]} \tag{15}$$

$$\frac{\partial \theta}{\partial \overline{t}} + \overline{v}\frac{\partial \theta}{\partial \overline{y}} = \frac{1}{\mathrm{Pr}}\left(1+\mathrm{N}\right)\frac{\partial^2 \theta}{\partial \overline{y}^2} + \frac{\delta}{\mathrm{Pr}}\theta + \mathrm{Ec}\left[\left(\frac{\partial \overline{u}}{\partial \overline{y}}\right)^2 + \left(\frac{\partial \overline{w}}{\partial \overline{y}}\right)^2\right] + \mathrm{Du}\frac{\partial^2 \phi}{\partial \overline{y}^2} + \mathrm{R}\frac{\left(h^2+1\right)}{\left[h^2 + \left(1+m^2\right)\right]}\left(\overline{u}^2 + \overline{w}^2\right) \tag{16}$$

$$\frac{\partial \phi}{\partial \overline{t}} + \overline{v}\frac{\partial \phi}{\partial \overline{y}} = \frac{1}{\mathrm{Sc}}\frac{\partial^2 \phi}{\partial \overline{y}^2} - \gamma\phi + \mathrm{Sr}\frac{\partial^2 \theta}{\partial \overline{y}^2} \tag{17}$$

$$\frac{\partial h}{\partial \overline{t}} = \frac{\partial \overline{u}}{\partial \overline{y}} + \frac{1}{\mathrm{R_m}}\frac{\partial^2 h}{\partial \overline{y}^2} \tag{18}$$

subject to the following initial and boundary conditions

$$\overline{u}(\overline{y}, 0) = 0,\ \overline{w}(y, 0) = 0,\ \theta(\overline{y}, 0) = 0,\ \phi(\overline{y}, 0) = 0,\ h(\overline{y}, 0) = 0 \tag{19}$$

$$\overline{u}(0, \overline{t}) = 1,\ \overline{w}(0, \overline{t}) = 0,\ \theta(0, \overline{t}) = 1, \phi(0, \overline{t}) = 1,\ h(0, \overline{t}) = 1 \tag{20}$$

$$\overline{u}(\infty, \overline{t}) = 0,\ \overline{w}(\infty, \overline{t}) = 0,\ \theta(\infty, \overline{t}) = 0,\ \phi(\infty, \overline{t}) = 0,\ h(\infty, \overline{t}) = 0 \tag{21}$$

2.2. Skin-Friction, Rates of Heat and Mass Transfer

The important parameters of engineering concern in this study are the skin-friction coefficient C_f, the local Nusselt number Nu_x and the local Sherwood number Sh_x. These parameters are defined as:

$$C_{f_x} = \frac{\tau_x}{\rho U_0^2}, \quad C_{f_z} = \frac{\tau_z}{\rho U_0^2} \tag{22}$$

$$\mathrm{Nu}_x = \frac{x q_{\mathrm{wall}}}{k(T_{\mathrm{wall}} - T_\infty)}, \quad \mathrm{Sh}_x = \frac{x J_{\mathrm{wall}}}{D_{\mathrm{m}}(C_{\mathrm{wall}} - C_\infty)} \tag{23}$$

The skin-friction coefficient, the local Nusset number and the local Sherwood number physically indicate the shear stress (or viscous drag per unit area), rate of heat transfer and rate of mass transfer at the plate, respectively. The shear stress components τ_x and τ_z, the heat flux q_{wall} and the mass flux J_{wall} at the plate are defined as

$$\tau_x = -\mu\left(\frac{\partial u}{\partial y}\right)_{y=0}, \tau_z = -\mu\left(\frac{\partial w}{\partial y}\right)_{y=0} \tag{24}$$

$$q_{\mathrm{wall}} = -k\left(\frac{\partial T}{\partial y}\right)_{y=0}, J_{\mathrm{wall}} = -D_{\mathrm{m}}\left(\frac{\partial C}{\partial y}\right)_{y=0} \tag{25}$$

The dimensionless form of equations (24) and (25) are given as:

$$\tau_x = -\rho U_0^2\left(\frac{\partial \bar{u}}{\partial \bar{y}}\right)_{\bar{y}=0} \quad \tau_z = -\rho U_0^2\left(\frac{\partial \bar{w}}{\partial \bar{y}}\right)_{\bar{y}=0} \tag{26}$$

$$q_{\mathrm{wall}} = -\frac{k\left(T_{\mathrm{wall}} - T_\infty\right)\rho U_0}{\mu}\left(\frac{\partial \theta}{\partial \bar{y}}\right)_{\bar{y}=0} \tag{27}$$

$$J_{\mathrm{wall}} = -\frac{D_{\mathrm{m}}\left(C_{\mathrm{wall}} - C_\infty\right)\rho U_0}{\mu}\left(\frac{\partial \phi}{\partial \bar{y}}\right)_{\bar{y}=0} \tag{28}$$

Substituting equations (26)—(28) into equations (22)—(23) and simplifying yields

$$C_{f_x} = -\left(\frac{\partial \bar{u}}{\partial \bar{y}}\right)_{\bar{y}=0}, \quad C_{f_z} = -\left(\frac{\partial \bar{w}}{\partial \bar{y}}\right)_{\bar{y}=0} \tag{29}$$

$$\mathrm{Nu}_x = -\mathrm{Re}_x\left(\frac{\partial \theta}{\partial \bar{y}}\right)_{\bar{y}=0}, \quad \mathrm{Sh}_x = -\mathrm{Re}_x\left(\frac{\partial \phi}{\partial \bar{y}}\right)_{\bar{y}=0} \tag{30}$$

where $\mathrm{Re}_x = \left(x\rho U_0\right)/\mu$ is the local Reynolds number.

The model equations (13)—(18) subject to the initial and boundary conditions (19)—(21) together with the skin-friction coefficients (29) and the rates of heat and mass transfer (30) are solved numerically by the finite difference method based on the forward-time central-space scheme.

3. Results and Discussion

The flow variables in this study are the primary velocity, secondary velocity, temperature, species concentration and magnetic induction. The various flow parameters that have been varied include the magnetic parameter (M^2), Hall parameter (m), Eckert number (Ec), Joule heating parameter (R), radiation parameter (N), chemical reaction parameter (γ), heat source parameter (δ), rotation parameter $(\mathrm{R_o})$, magnetic Reynolds number $(\mathrm{R_m})$, Dufour number (Du), Soret number (Sr), Schmidt number (Sc), Prandtl number (Pr), thermal Grashof number $(\mathrm{Gr_T})$, mass Grashof number $(\mathrm{Gr_C})$, and suction parameter $(\bar{v}_0)$, at time $t = 0.1887$. These parameters are input into a computer program where each parameter is varied at a time.

3.1. Effects of Varying Eckert Number

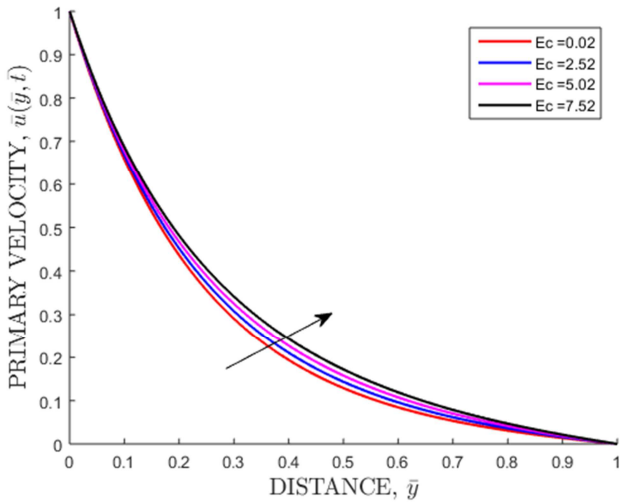

(a) Primary Velocity Profiles

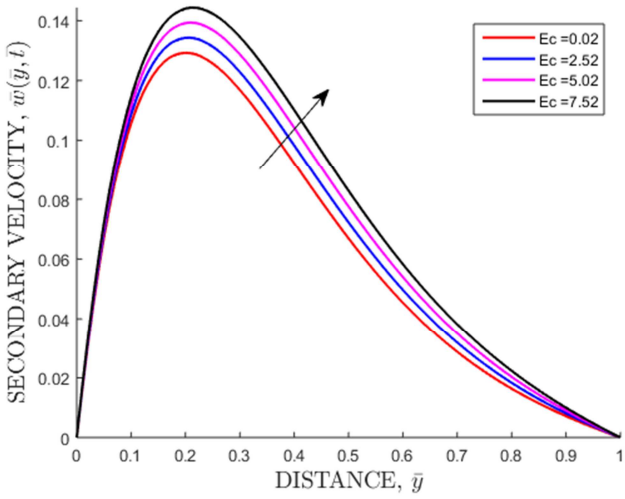

(b) Secondary Velocity Profiles

Figure 2. *Velocity profiles for different values of Eckert number.*

Figure 2 shows that an increase in Eckert number leads to an increase in both the primary and secondary velocity profiles. Figure 3 shows that an increase in Eckert number leads to an increase in the temperature profiles. Figure 4 shows that an increase in Eckert number leads to a decrease in the concentration profiles. The Eckert number expresses the relationship between the kinetic energy in the flow and the enthalpy. It embodies the conversion of kinetic energy into internal energy by work done against the viscous fluid stresses. Thus, an increase in Eckert number means the fluid absorbs more heat energy that is released from the internal viscous forces. This in turn increases the temperature and the velocity of the convection currents due to increased thermal buoyancy forces respectively. Higher velocity profiles imply an increased rate of species transportation away from the boundary layer region, and hence the observed decrease in the concentration profiles. A positive Eckert number implies cooling of the plate or heating the fluid. This causes a rise in the temperature and the velocity of the fluid respectively. The observed increase in temperature profiles is because of the energy generated due to frictional heating in the boundary layer.

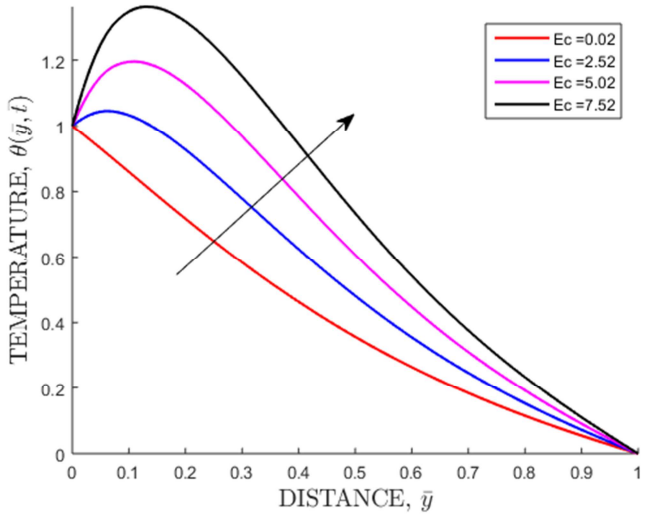

Figure 3. *Temperature profiles for different values of Eckert number.*

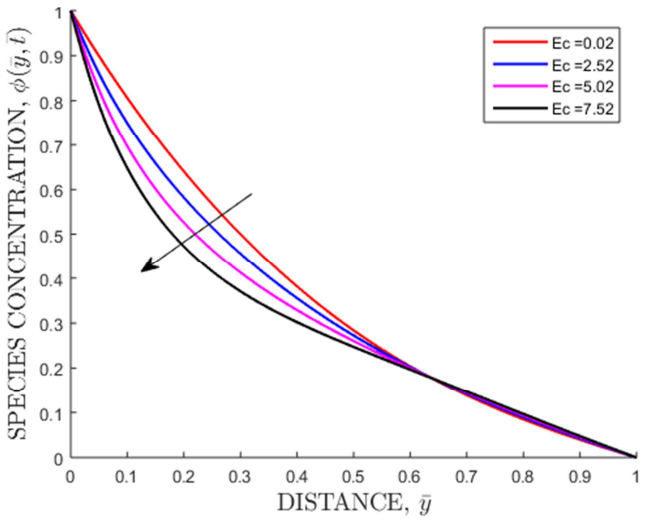

Figure 4. *Concentration profiles for different values of Eckert number.*

3.2. Effects of Varying Prandtl Number

Figure 5 shows that an increase in the Prandtl number leads to a decrease in both the primary and secondary velocity profiles. Figure 6 shows that an increase in the Prandtl number leads to a decrease in the temperature profiles. Figure 7 shows that an increase in the Prandtl number leads to an increase in the concentration profiles. The observed decrease in temperature profiles is due to the fact that thermal conductivity of the fluid decreases with increasing, resulting a decrease in thermal boundary layer thickness. An increase in the Prandtl number results in a decrease of the thermal boundary layer thickness and in general, lower average temperature within the boundary layer. The reason is that smaller values of are equivalent to increasing the thermal conductivities and therefore, heat is able to diffuse away from the heated surface more rapidly than for higher values of Pr. Hence, in the case of smaller Prandtl numbers, as the boundary layer becomes thicker, the rate of heat transfer reduces.

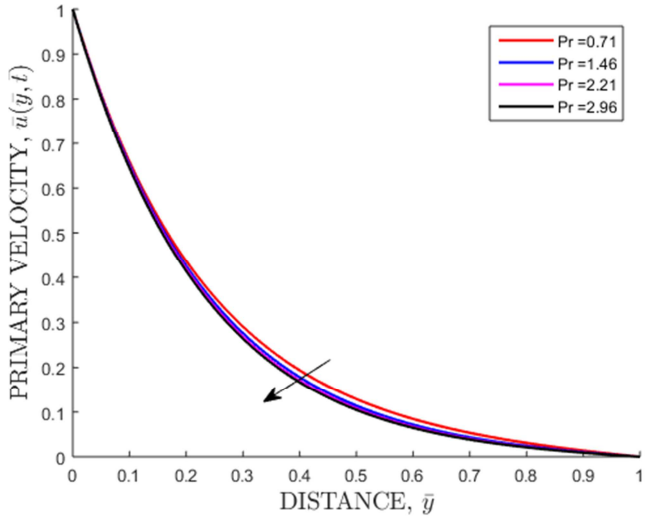

(a) Primary Velocity Profiles

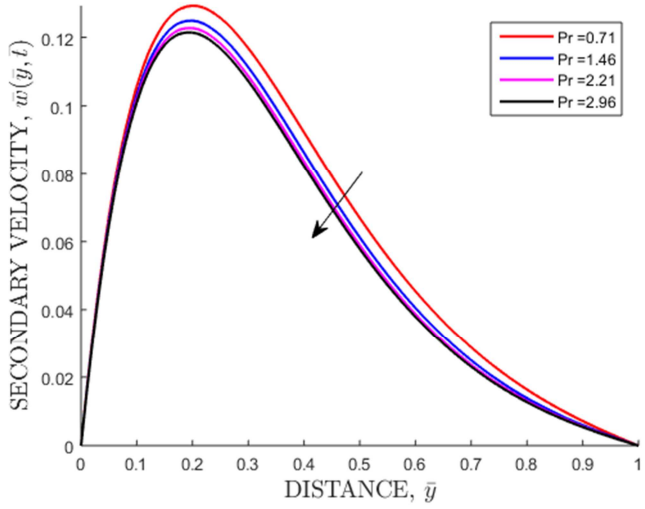

(b) Secondary Velocity Profiles

Figure 5. *Velocity profiles for different values of Prandtl number.*

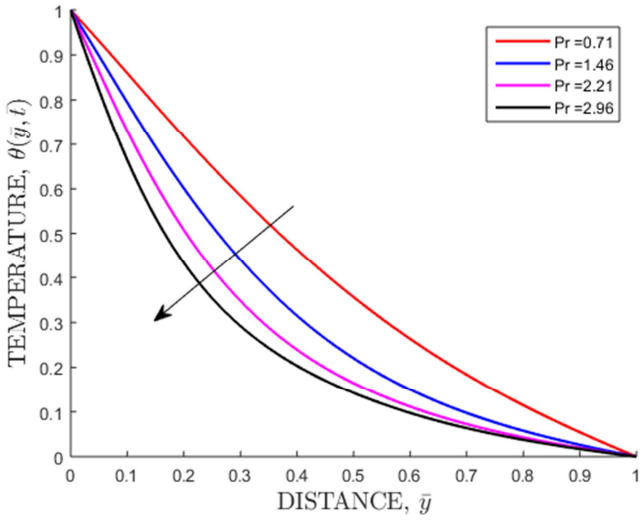

Figure 6. *Temperature profiles for different values of Prandtl number.*

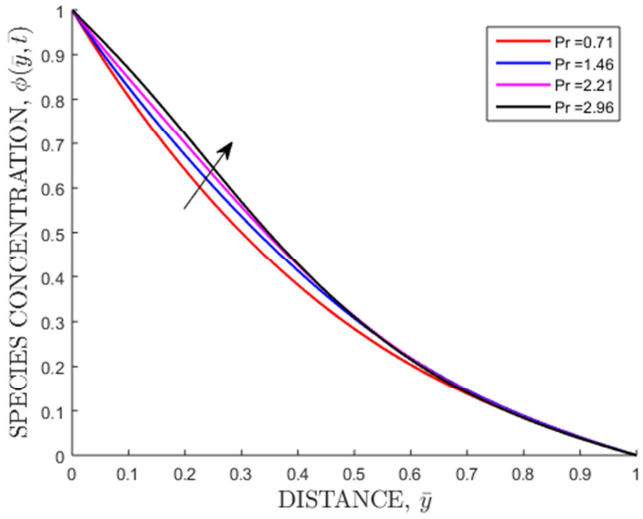

Figure 7. *Concentration profiles for different values of Prandtl number.*

3.3. Effects of Varying Schmidt Number

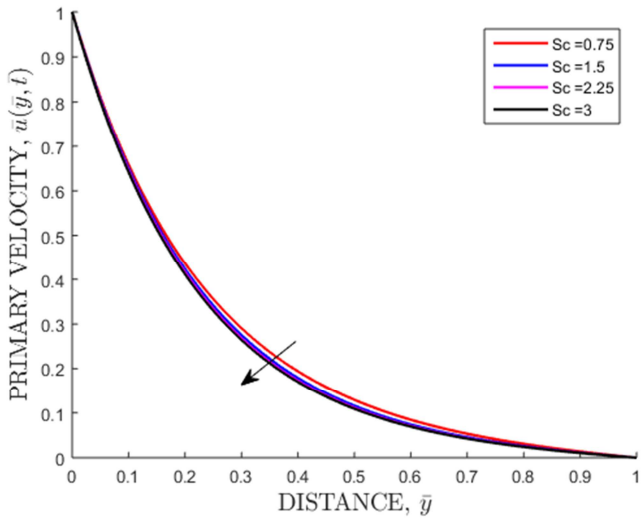

(a) Primary Velocity Profiles

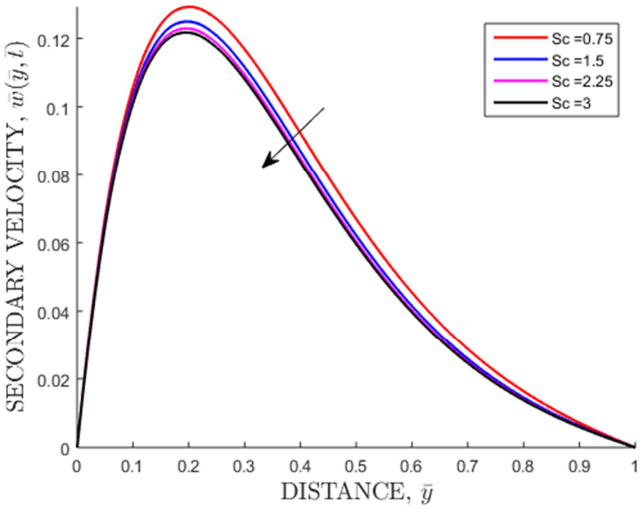

(b) Secondary Velocity Profiles

Figure 8. *Velocity profiles for different values of Schmidt number.*

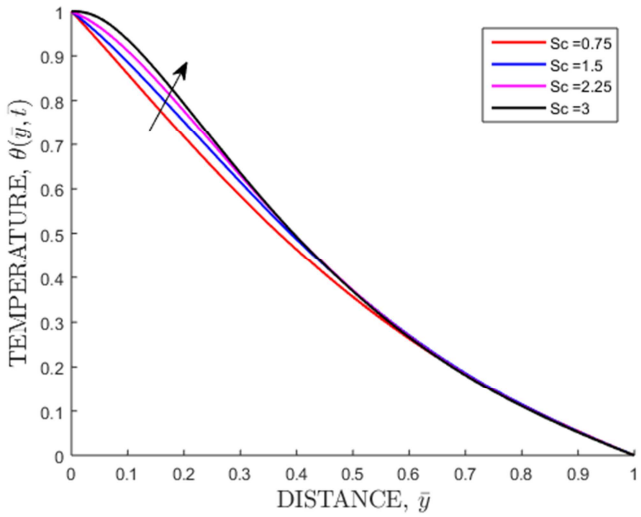

Figure 9. *Temperature profiles for different values of Schmidt number.*

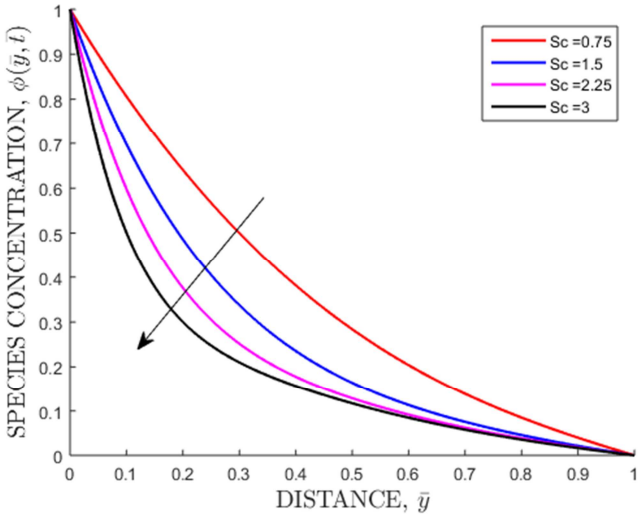

Figure 10. *Concentration profiles for different values of Schmidt number.*

Figure 8 shows that an increase in Schmidt number leads to a decrease in both the primary and secondary velocity profiles. Figure 9 shows that an increase in Schmidt number leads to an increase in the temperature profiles near the plate. Figure 10 shows that an increase in Schmidt number leads to a decrease in the concentration profiles. The reasons behind the observations are that increasing Schmidt number results in thickening of the thermal boundary layer and thinning of the concentration boundary layer. Increasing Schmidt number implies that viscous forces dominate over the diffusional effects. Therefore, an increase in Schmidt number will counteract momentum diffusion since viscosity effects will increase and molecular diffusivity will be reduced. Thus, the flow will be decelerated with a rise in Schmidt number. The Schmidt number embodies the ratio of the momentum diffusivity to the mass (species) diffusivity. It physically relates the relative thickness of the hydrodynamic boundary layer and mass transfer (concentration) boundary layer. As the Schmidt number increases, the concentration decreases. This causes the concentration buoyancy effects to decrease yielding a reduction in the fluid velocity. The reductions in the velocity and concentration profiles are accompanied by simultaneous reductions in the velocity and concentration boundary layers.

3.4. Effects of Varying Heat Source Parameter

Figure 11 shows that an increase in the heat source parameter leads to a decrease in both primary and secondary velocity profiles. Figure 12 shows that increase in the heat source parameter leads to a decrease in the temperature profiles. Figure 13 shows that increase in the heat source parameter leads to an increase in the concentration profiles. The presence of a heat source produces a cooling effect that decreases velocity of the convection currents that move upwards next to the plate, leading to higher concentration profiles. Thus, the presence of heat source generates energy in the boundary layer that causes the increase in fluid temperature.

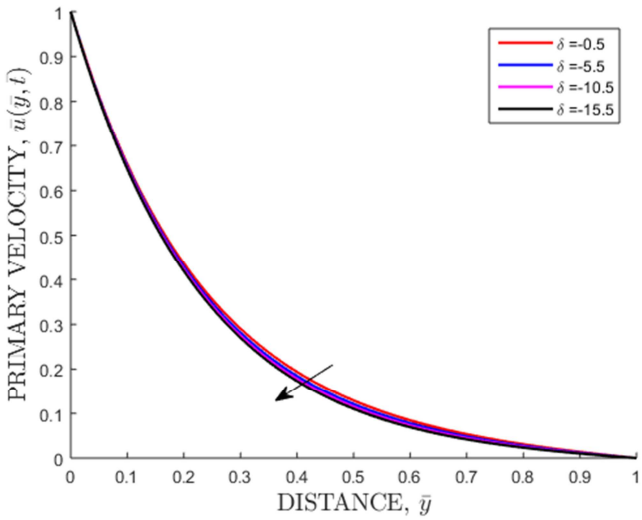

(a) Primary Velocity Profiles

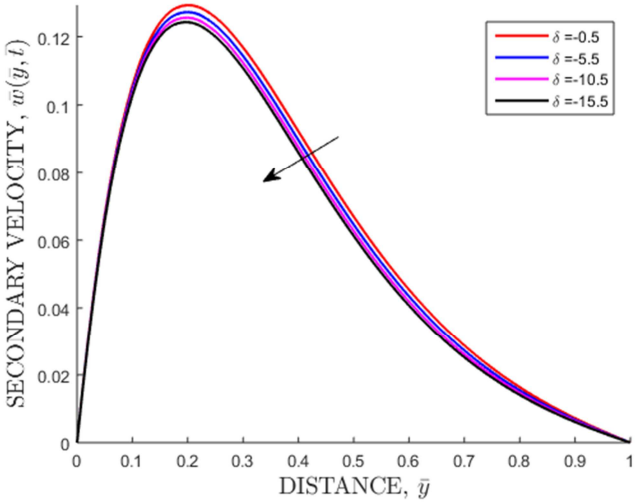

(b) Secondary Velocity Profiles

Figure 11. *Velocity profiles for different values of heat source parameter.*

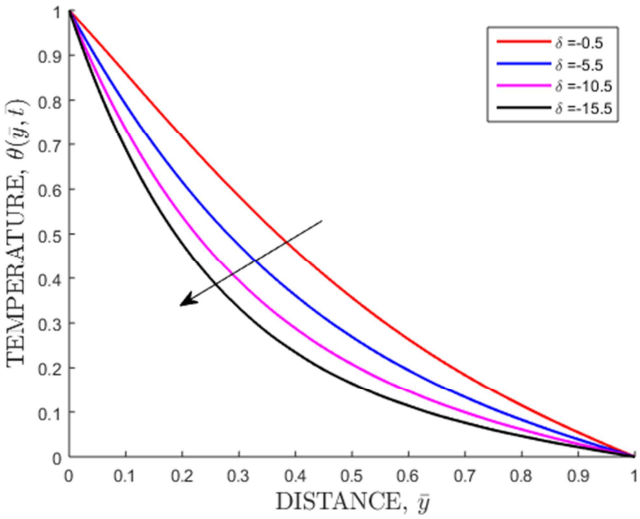

Figure 12. *Temperature profiles for different values of heat source parameter.*

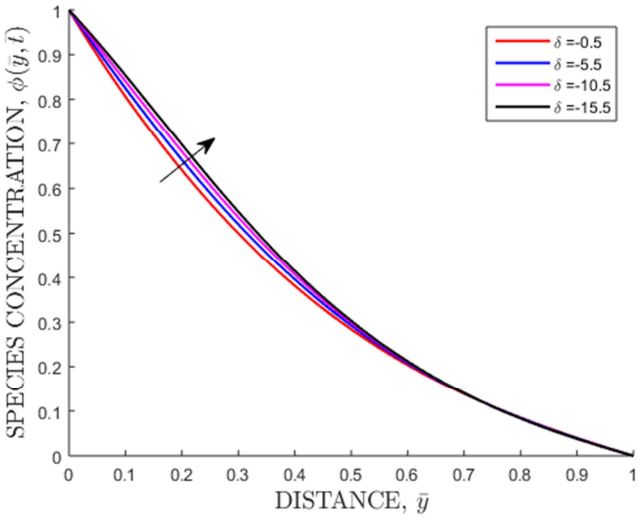

Figure 13. *Concentration profiles for different values of heat source parameter.*

3.5. Effects of Varying Radiation Parameter

Figure 14 shows that an increase in radiation parameter leads to an increase in the temperature profiles. Therefore, radiation can be used to control the fluid temperature. The effect of radiation parameter is to decrease the rate of energy transport to the fluid and thereby decreasing the temperature of the fluid.

3.6. Skin-Friction Coefficient and Rates of Heat and Mass Transfer

The local skin-friction coefficients, the local Nusselt number and local sherwood number are computed for $\mathrm{Du}=0.5$, $\mathrm{Gr_T}=5.0$, $\mathrm{Gr_C}=5.0$, $\mathrm{K}=10^3$, $\mathrm{N}=0.25$, $\mathrm{Pr}=0.71, \mathrm{Rm}=1.5$, $\mathrm{Sc}=0.75$, $\mathrm{Sr}=0.5$, $\delta=-0.5, \gamma=0.5$. The parameters $\mathrm{M}, \mathrm{m}, \mathrm{Ec}$, $\mathrm{R_o}, \mathrm{R}$, and $\bar{v}_0$ are varied on the local coefficients of skin-friction, local Nusselt number and local Sherwood number and the numerical values of C_{f_x} , C_{f_z} , $\mathrm{Nu}_x\mathrm{Re}_x^{-1}$ and $\mathrm{Sh}_x\mathrm{Re}_x^{-1}$ are presented in Table 1.

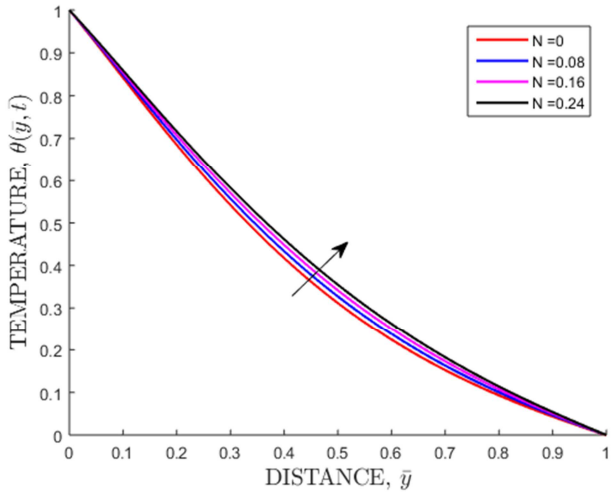

Figure 14. *Temperature profiles for different values of radiation parameter.*

Table 1. *Values of skin-friction coefficient and rates of heat and mass transfer for various values of the parameters* M, m, Ec, R_O, R *, and* $\bar{v}_0$.

M	m	Ec	$\mathrm{R_o}$	R	$\bar{v}_0$	C_{f_x}	C_{f_z}	$\mathrm{Nu}_x\mathrm{Re}_x^{-1}$	$\mathrm{Sh}_x\mathrm{Re}_x^{-1}$
5	0.5	0.02	3	5	1	3.7855	-1.3458	1.3823	2.0174
8	0.5	0.02	3	5	1	6.1116	-1.3859	1.4584	1.9962
11	0.5	0.02	3	5	1	8.0485	-1.3993	1.4949	1.9856
14	0.5	0.02	3	5	1	9.6660	-1.4025	1.5136	1.9803
5	1	0.02	3	5	1	3.3421	-1.9080	1.4250	2.0040
5	1.5	0.02	3	5	1	2.8474	-2.1600	1.4665	1.9912
5	2	0.02	3	5	1	2.4363	-2.2172	1.4988	1.9817
5	0.5	2.52	3	5	1	3.6792	-1.3772	-0.8812	2.7963
5	0.5	5.02	3	5	1	3.5773	-1.4078	-2.9876	3.5212
5	0.5	7.52	3	5	1	3.4793	-1.4379	-4.9504	4.1966
5	0.5	0.02	4.5	5	1	3.8870	-1.5901	1.3848	2.0177
5	0.5	0.02	6	5	1	4.0015	-1.8214	1.3876	2.0179
5	0.5	0.02	7.5	5	1	4.1272	-2.0388	1.3907	2.0181
5	0.5	0.02	3	15	1	3.7709	-1.3491	0.9811	2.1469
5	0.5	0.02	3	25	1	3.7562	-1.3524	0.5766	2.2771
5	0.5	0.02	3	35	1	3.7413	-1.3557	0.1687	2.4082
5	0.5	0.02	3	5	2	4.4694	-1.2657	1.7440	2.5220
5	0.5	0.02	3	5	3	5.2190	-1.1614	2.1383	3.0767
5	0.5	0.02	3	5	4	6.0185	-1.0421	2.5609	3.6683

From Table 1, the following observations are noted:

i. Increase in the magnetic parameter results in an increase in the primary coefficient of skin-friction (C_{f_x}), the magnitude of the secondary coefficient of skin-friction (C_{f_z}), and Nusselt number (Nu_x); but to a decrease in the Sherwood number (Sh_x). The skin-friction coefficient is proportional to velocity and since both velocity profiles decrease with increase in magnetic parameter, the wall shear stress is expected to increase due to increase in the Lorentz force that decreases the velocity of the fluid. Thermal boundary layer thickness decreases with increase in magnetic parameter resulting in the observed increase in the Nusselt number. The observed decrease in the Sherwood number is attributed to the fact that increasing the values of magnetic parameter causes thinning of the concentration boundary layer, resulting in a higher rate of transportation of the species in the concentration boundary layer.

ii. Similarly, an increase in the Hall parameter results in an increase in the primary coefficient of skin-friction, the magnitude of the secondary coefficient of skin-friction, and Nusselt number; but to a decrease in the Sherwood number. Increase in Hall parameter increases the Joule heating since the conductivity of the fluid decreases, leading to a thicker thermal boundary layer. This leads to a reduced rate of heat transfer.

iii. Increase in the Eckert number leads to a decrease in the coefficients of skin-friction and Nusselt number; but to an increase in the Sherwood number. Increasing the value of Eckert number leads to an increase in the velocity of the fluid and hence the observed increase in

the values of both the wall shear stresses. Increase in Eckert number translates to a lower value of the temperature difference, and to a reduced rate of heat transfer. This in turn enhances the rate of species transportation leading to increase in Sherwood number. A positive Eckert number implies cooling of the plate thereby enhancing convection currents leading to increased velocity and the temperature of the fluid. The resulting thicker thermal boundary layer leads to a reduced rate of heat transfer.

iv. Increase in the rotation parameter leads to an increase in the primary coefficient of skin-friction, magnitude of the secondary coefficient of skin-friction, Nusselt number and Sherwood number. The explanations are that increasing the values of rotation parameter causes an increase in the magnitude of the secondary velocity profiles that in turn leads to an increase in the magnitude of the secondary coefficient of skin-friction. Further, increasing the values of rotation parameter leads to a thinner thermal boundary layer and hence enhancing the rate of heat transfer. Decrease in the primary velocity profiles leads to a reduced rate of transportation of species away from the plate, leading to the observed increase in the value of Sherwood number.

v. Increase in the joule heating parameter leads to a decrease in the coefficients of skin-friction and Nusselt number; but to an increase in the Sherwood number. This is attributed to the fact that the effect of Joule heating is to decrease the rate of energy transport to the fluid, thereby decreasing the temperature of the fluid. Increase in the velocity of the fluid leads to an increase in the values of skin-friction coefficients, that in turn lead to a decrease in the species concentration.

vi. Increase in the suction parameter leads to an increase in the coefficients of skin-friction, Nusselt number and Sherwood number. Suction decelerates the velocity of the fluid particles leading to lower flow velocities. Thermal boundary layer thickness decreases with increase in suction parameter, leading to an increased rate of heat transfer. Decrease in concentration boundary layer thickness leads to an increased rate of species transportation, and hence to increase in the Sherwood number.

4. Conclusion

The FTCS schemes used in the computations in this study are stable and consistent. The effects of various flow parameters on unsteady hydromagnetic Stokes free convection flow of a viscous, incompressible and electrically conducting fluid past an impulsively started infinite vertical porous plate subjected to variable suction in a rotating system with heat and mass transfer in the presence of a strong, non-uniform magnetic field normal to the plate have been investigated by varying the parameters. The local rates of heat and mass transfer, and the coefficients of friction due to the primary and the secondary flow fields have also been determined. The important findings in this study are:

i. Radiation can be used to control the velocity, concentration and thermal boundary layers of flow in porous media quite effectively.

ii. Varying the Prandtl number can be used to control the fluid's flow velocity, temperature, concentration, sheer stress, and the rates of heat and mass transfer respectively.

iii. The Hall effects can be utilized in controlling the fluid's velocity, concentration, temperature and sheer stress and the rates of heat and mass transfer respectively.

iv. Varying the value of the Heat source parameter can be used to control the shear stresses, rate of heat transfer and rate of mass transfer respectively.

Acknowledgements

The authors would like to thank the academic and technical support of Jomo Kenyatta University of Agriculture and Technology (JKUAT) especially Kisii CBD campus for providing the necessary learning resources to facilitate the successful completion of this research project. The library, computer and other facilities of the University have been indispensable. Augustine Mayaka thanks the chairman, members of staff in the department of pure and applied mathematics and his colleagues for their support and making his stay in the department pleasant and memorable.

References

[1] O. D. Makinde and A. Ogulu, "The effect of thermal radiation on the heat and mass transfer flow of a variable viscosity fluid past a vertical porous plate permeated by a transverse magnetic field," Chemical Engineering Communications, vol. 195, no. 12, pp. 1575–1584, 2008.

[2] J. Prakash, D. Bhanumathi, A. V. Kumar, and S. Varma, "Diffusionthermo and radiation effects on unsteady mhd flow through porous medium past an impulsively started infinite vertical plate with variable temperature and mass diffusion," Transport in porous media, vol. 96, no. 1, pp. 135–151, 2013.

[3] M. Narahari, S. Tippa, and R. Pendyala, "Unsteady magnetohydrodynamic free convection flow of a radiative fluid past an infinite vertical plate with constant heat and mass flux," in Applied Mechanics and Materials, vol. 465. Trans Tech Publ, 2014, pp. 149–154.

[4] M. R. Murthy, R. S. Raju, and J. A. Rao, "Heat and mass transfer effects on mhd natural convective flow past an infinite vertical porous plate with thermal radiation and hall current," Procedia Engineering, vol. 127, pp. 1330–1337, 2015.

[5] R. S. Raju, "Combined influence of thermal diffusion and diffusion thermo on unsteady mhd free convective fluid flow past an infinite vertical porous plate in presence of chemical reaction," Journal of The Institution of Engineers (India): Series C, vol. 97, no. 4, pp. 505–515, 2016.

[6] J. Pattnaik, G. Dash, and S. Singh, "Diffusion-thermo effect with hall current on unsteady hydromagnetic flow past an infinite vertical porous plate," Alexandria Engineering Journal, vol. 56, no. 1, pp. 13–25, 2017.

[7] M. V. Krishna, M. G. Reddy, and A. Chamkha, "Heat and mass transfer on mhd rotating flow of second grade fluid past an infinite vertical plate embedded in uniform porous medium with hall effects," in Applied Mathematics and Scientific Computing. Springer, 2019, pp. 417–427.

[8] F. O. Ochieng, "Hydromagnetic jeffery-hamel unsteady flow of a dissipative non-newtonian fluid with nonlinear viscosity," Ph.D. dissertation, JKUAT-PAUSTI, 2018.

[9] B. Parent, M. N. Shneider, and S. O. Macheret, "Generalized ohms law and potential equation in computational weakly-ionized plasmadynamics," Journal of Computational Physics, vol. 230, no. 4, pp. 1439–1453, 2011.

[10] M. Kinyanjui, M. Emmah, J. Marigi, and K. Kwanza, "Hydromagnetic turbulent flow of a rotating system past a semiinfinite vertical plate with hall current.," International Journal of Heat and Mass transfer, vol. 79, pp. 97–119, 2012.

[11] M. Moorthy and K. Senthilvadivu, "Soret and dufour effects on natural convection flow past a vertical surface in a porous medium with variable viscosity," Journal of Applied Mathematics, vol. 2012, 2012.

[12] K. Giterere, "Magnetohydrodynamic flow in porous media over a stretching surface in a rotating system with heat and mass transfer," Ph.D. dissertation, 2013.

[13] A. Maguna and N. Mutua, "Hall current effects on free convection flow and mass transfer past semi-infinite vertical flat plate," Int. Jnl. of Mathematics and Statistics Studies, vol. 1, no. 4, pp. 1–22, 2013.

[14] H. Zaman, A. Sohail et al., "Stokes first problem for an unsteady mhd third-grade fluid in a non-porous half space with hall currents," Open Journal of Applied Sciences, vol. 2014, 2014.

[15] N. Marneni, S. Tippa, and R. Pendyala, "Ramp temperature and dufour effects on transient mhd natural convection flow past an infinite vertical plate in a porous medium," The European Physical Journal Plus, vol. 130, no. 12, p. 251, 2015.

[16] K. Subbanna, S. G. Mohiddin, and R. B. Vijaya, "Combined effects on mhd flow of newtonian fluid past infinite vertical porous plate," in AIP Conference Proceedings, vol. 1953, no. 1. AIP Publishing LLC, 2018, p. 140099.